

Direct numerical simulation of turbulent heat transfer in annuli: Effect of heat flux ratio

Meryem Ould-Rouiss, L. Redjem Saad, Guy Lauriat

► **To cite this version:**

Meryem Ould-Rouiss, L. Redjem Saad, Guy Lauriat. Direct numerical simulation of turbulent heat transfer in annuli: Effect of heat flux ratio. *International Journal of Heat and Fluid Flow*, Elsevier, 2009, 30 (4), pp.579-589. 10.1016/j.ijheatfluidflow.2009.02.018 . hal-00734060

HAL Id: hal-00734060

<https://hal-upec-upem.archives-ouvertes.fr/hal-00734060>

Submitted on 21 Sep 2012

HAL is a multi-disciplinary open access archive for the deposit and dissemination of scientific research documents, whether they are published or not. The documents may come from teaching and research institutions in France or abroad, or from public or private research centers.

L'archive ouverte pluridisciplinaire **HAL**, est destinée au dépôt et à la diffusion de documents scientifiques de niveau recherche, publiés ou non, émanant des établissements d'enseignement et de recherche français ou étrangers, des laboratoires publics ou privés.

List of Figures

1	Schematic of the computational domain.	18
2	Two-point correlations in the axial direction.	19
3	Two-point correlations in the azimuthal direction.	20
4	Mean velocity profile.	21
5	RMS velocity fluctuations: (a) streamwise, (b) radial, (c) azimuthal.	22
6	Positions of zero total shear stress r_0 and maximum velocity r_{max}	23
7	Mean temperature profiles. (a) inner cylinder, (b) outer cylinder	24
8	RMS of temperature fluctuations for $q^* = 1$	25
9	RMS of temperature fluctuations for various heat flux ratios. (a) $q^* \leq 1$, (b) $q^* \geq 1$	26
10	Turbulent heat fluxes for $q^* = 1$. (a) streamwise component, (b) wall-normal component	27
11	Streamwise turbulent heat flux for various heat flux ratios. (a) $q^* \leq 1$, (b) $q^* \geq 1$	28
12	Wall-normal turbulent heat flux for various heat flux ratios. (a) $q^* \leq 1$, (b) $q^* \geq 1$	29
13	Position of zero wall-normal turbulent heat flux versus heat flux ratio.	30

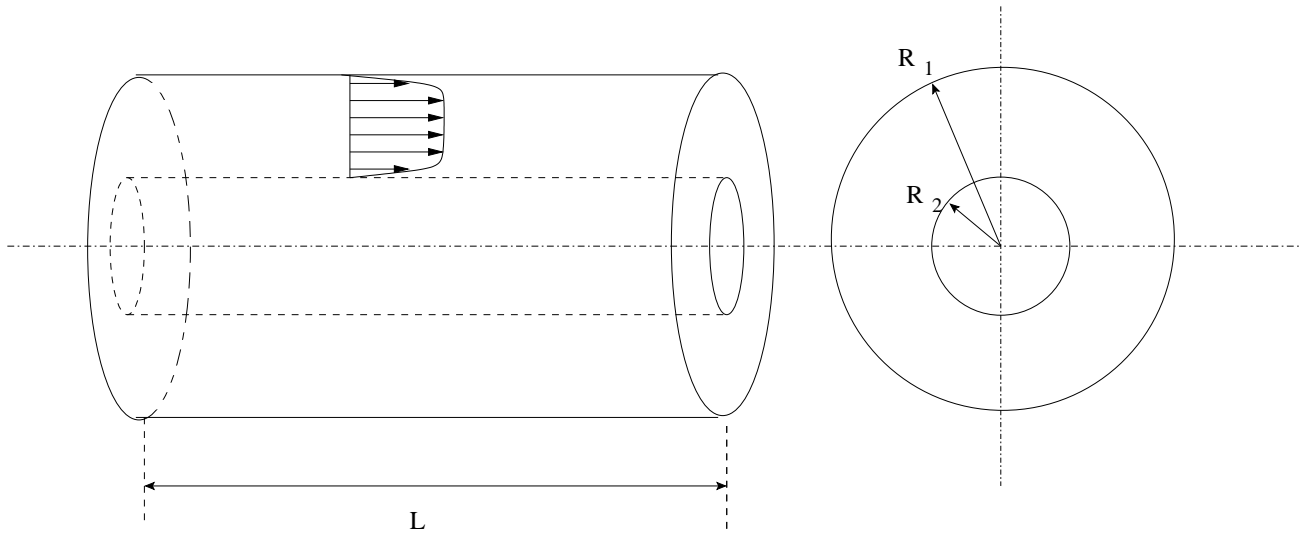


Figure 1: Schematic of the computational domain.

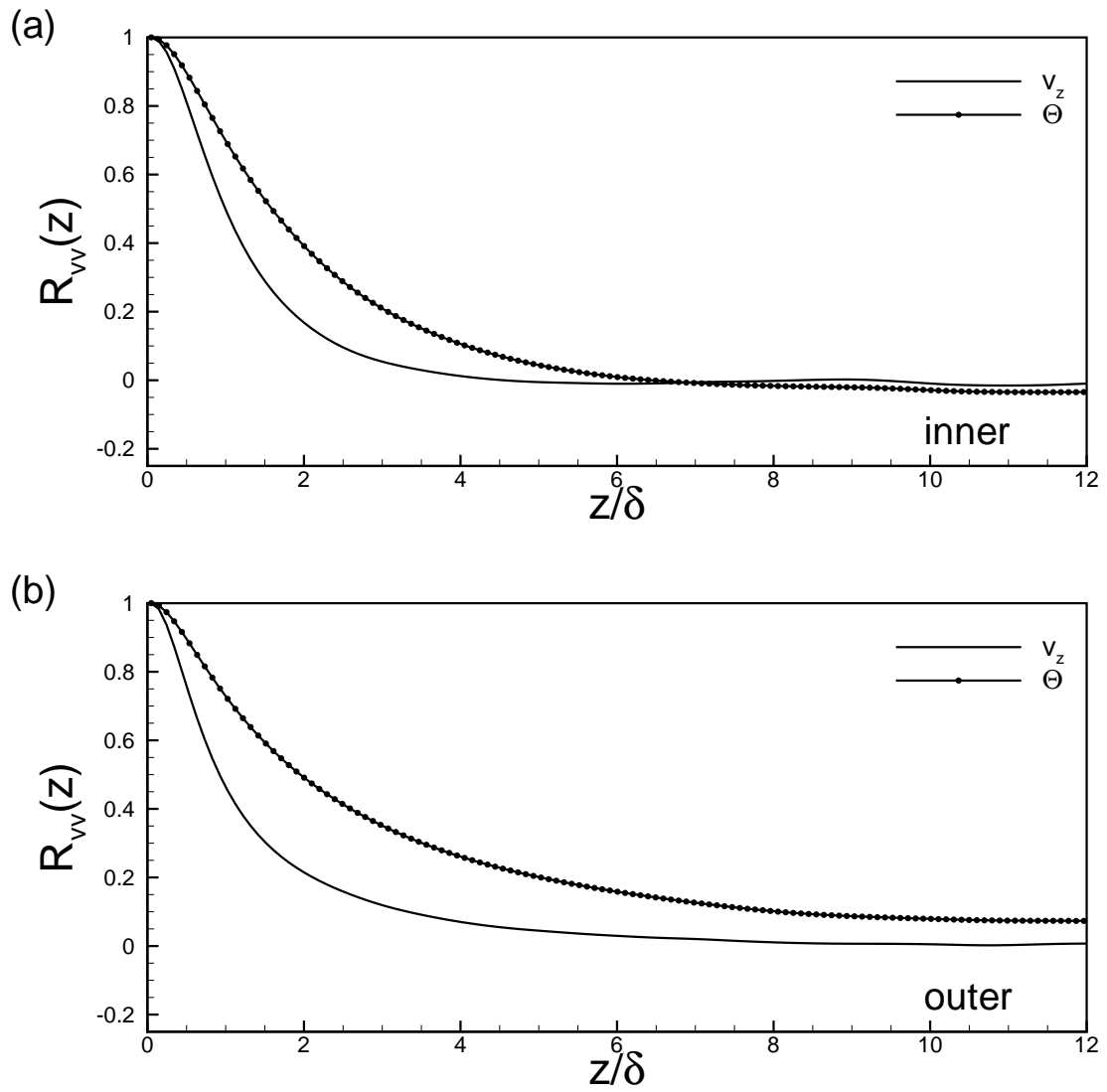


Figure 2: Two-point correlations in the axial direction.

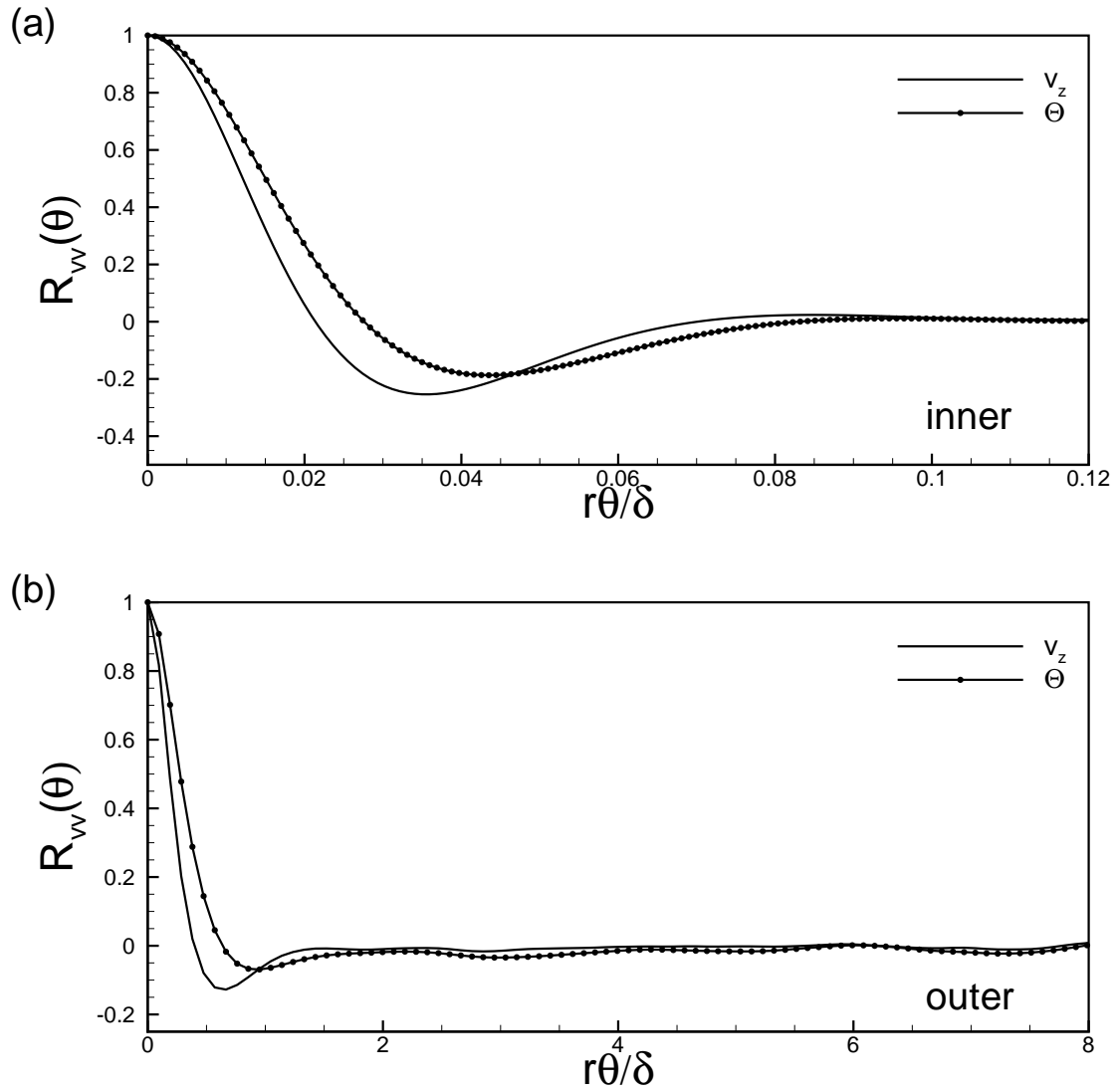


Figure 3: Two-point correlations in the azimuthal direction.

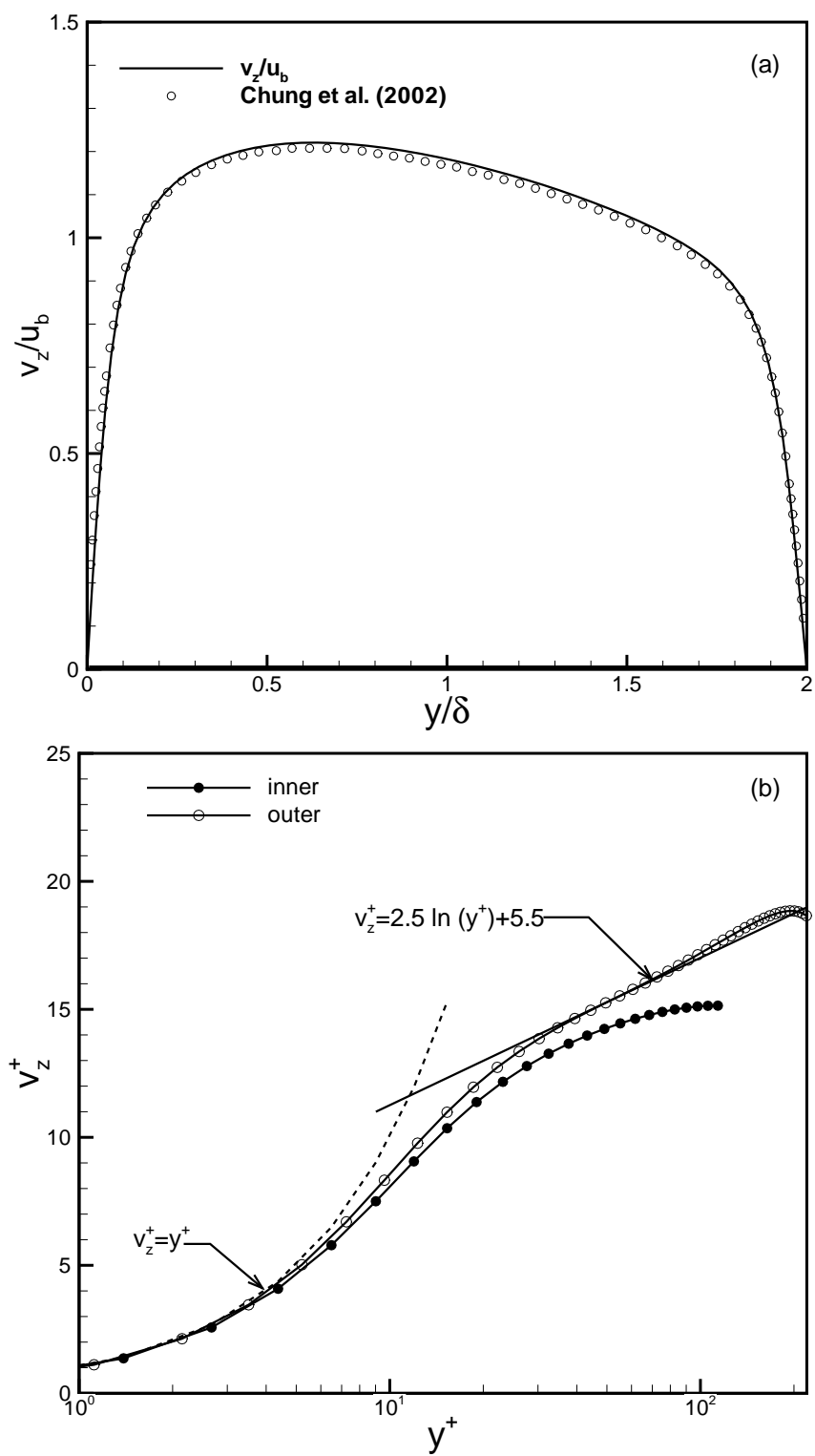


Figure 4: Mean velocity profile.

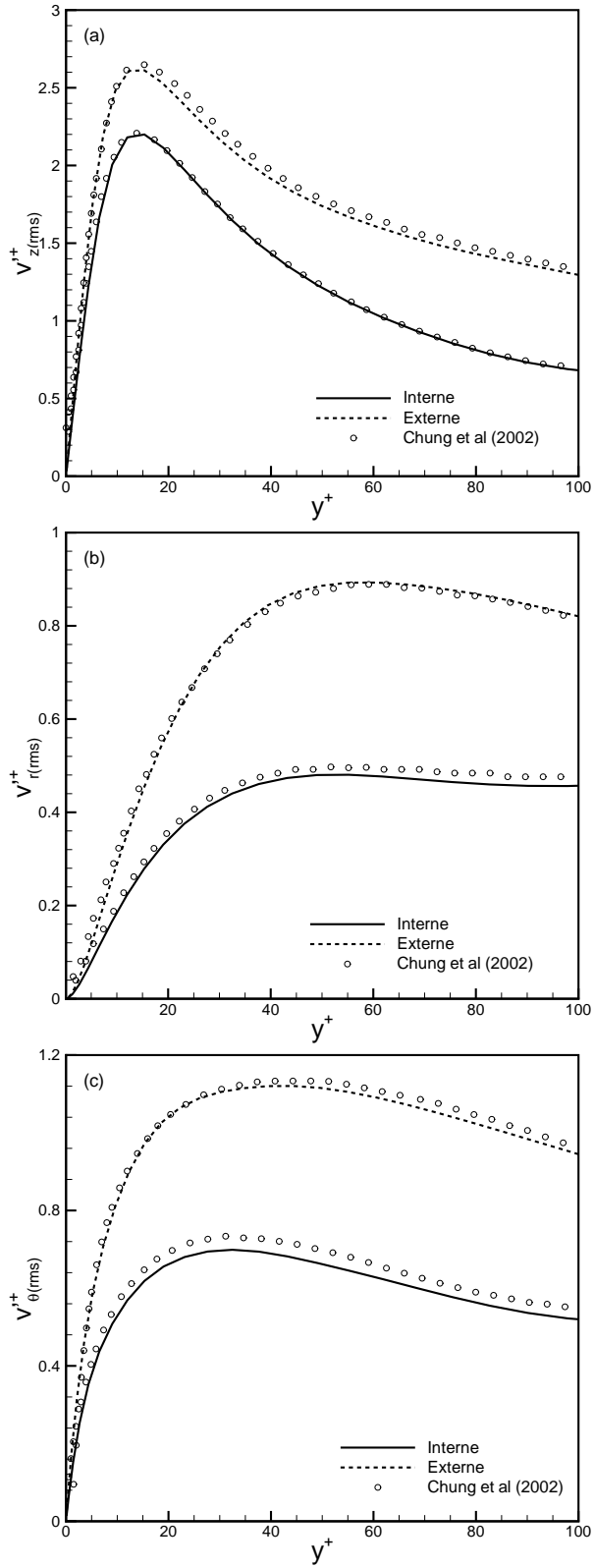


Figure 5: RMS velocity fluctuations: (a) streamwise, (b) radial, (c) azimuthal.

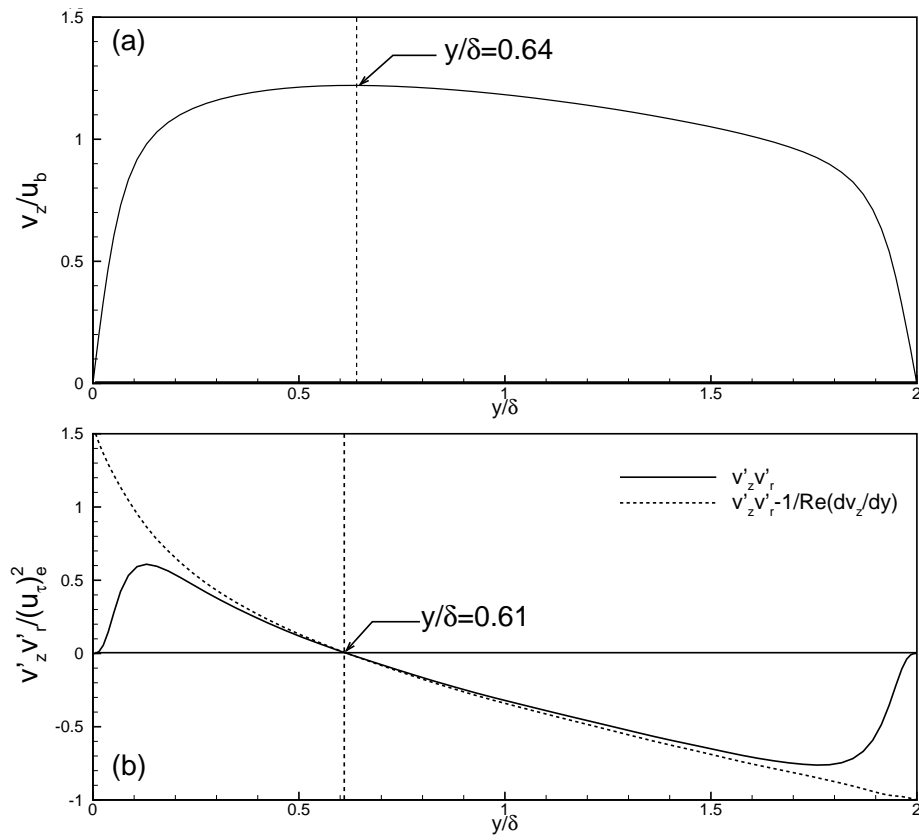


Figure 6: Positions of zero total shear stress r_0 and maximum velocity r_{max} .

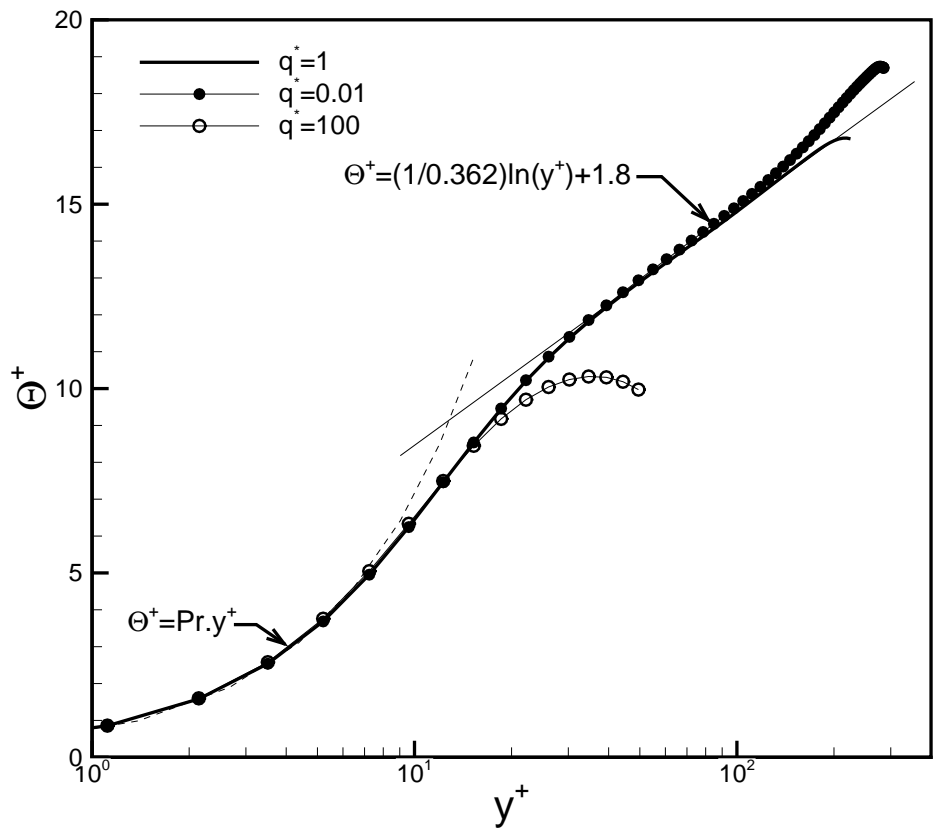
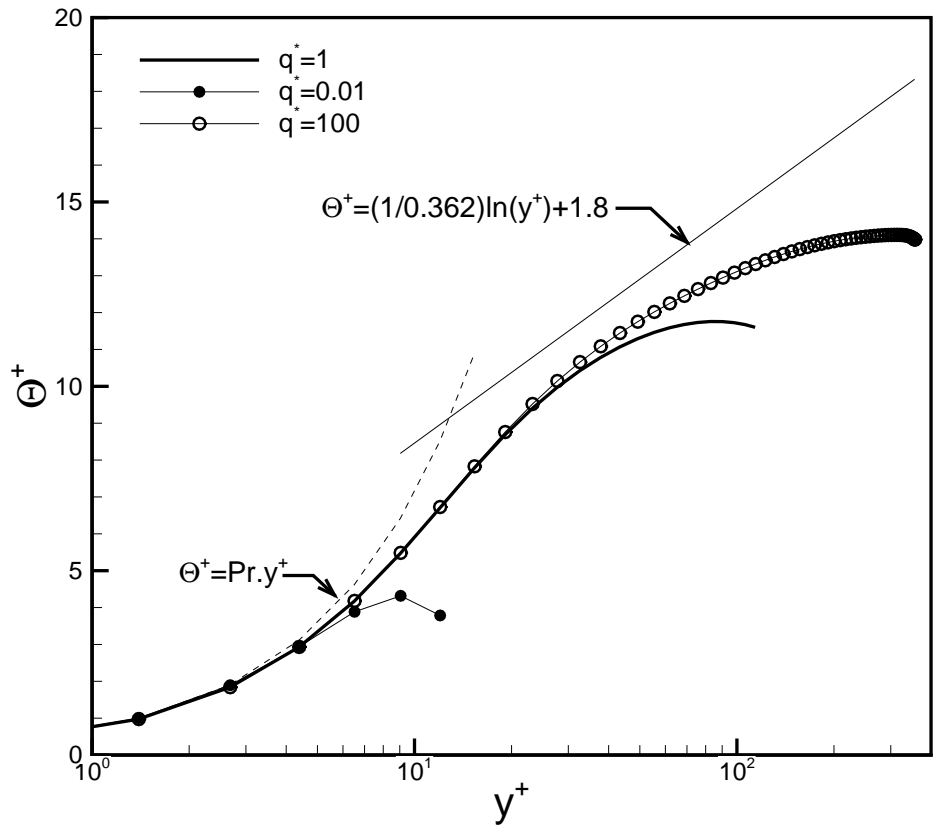


Figure 7: Mean temperature profiles. (a) inner cylinder, (b) outer cylinder

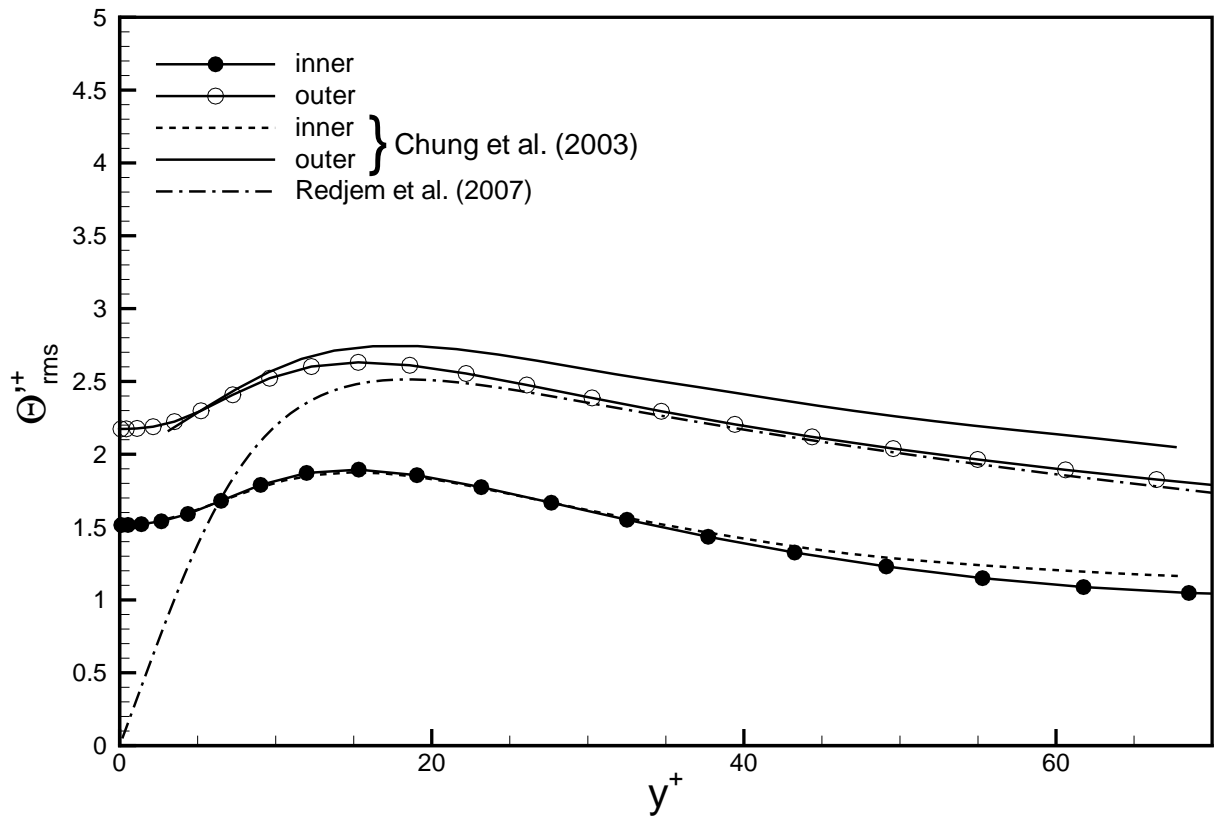


Figure 8: RMS of temperature fluctuations for $q^* = 1$.

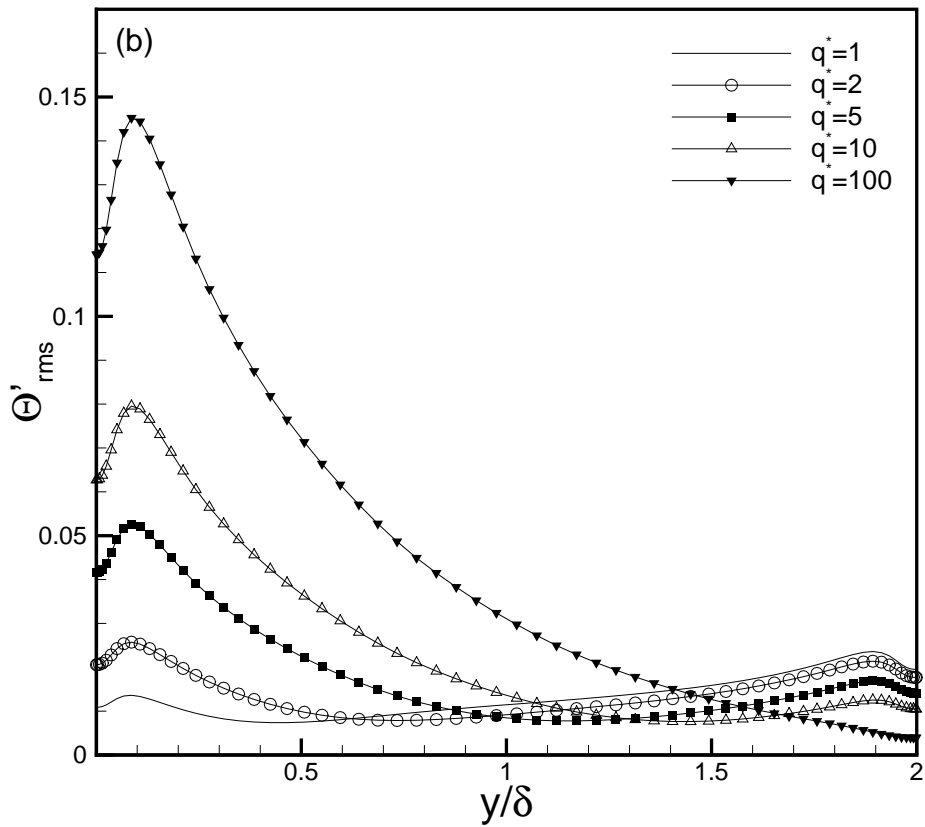
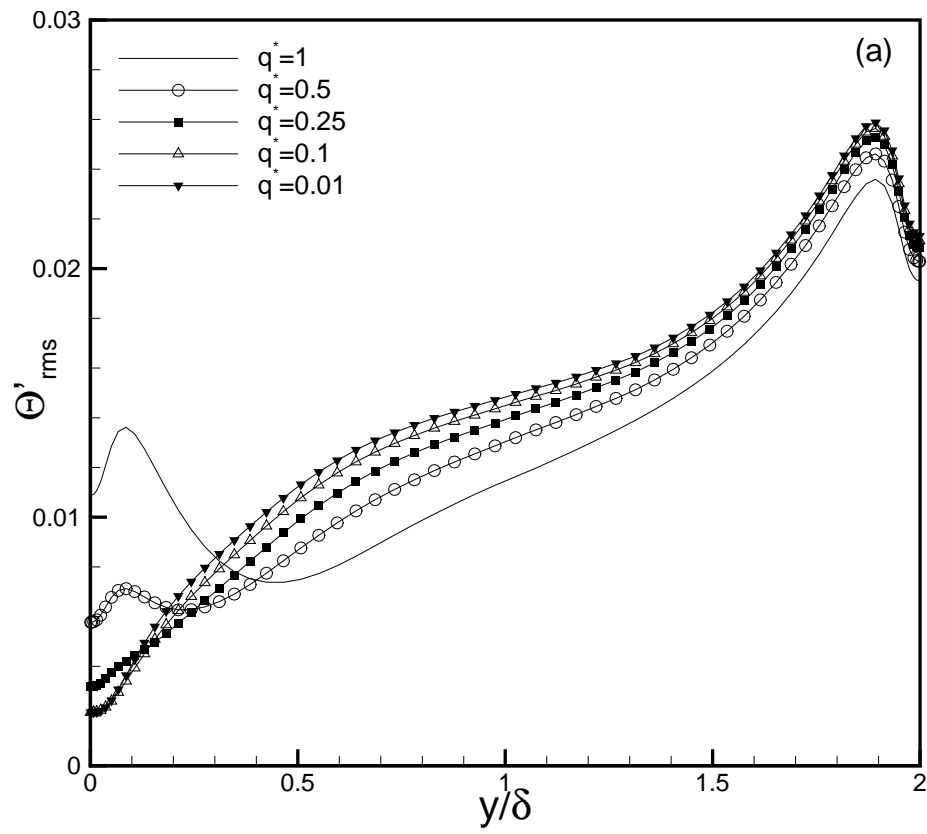


Figure 9: RMS of temperature fluctuations for various heat flux ratios. (a) $q^* \leq 1$, (b) $q^* \geq 1$

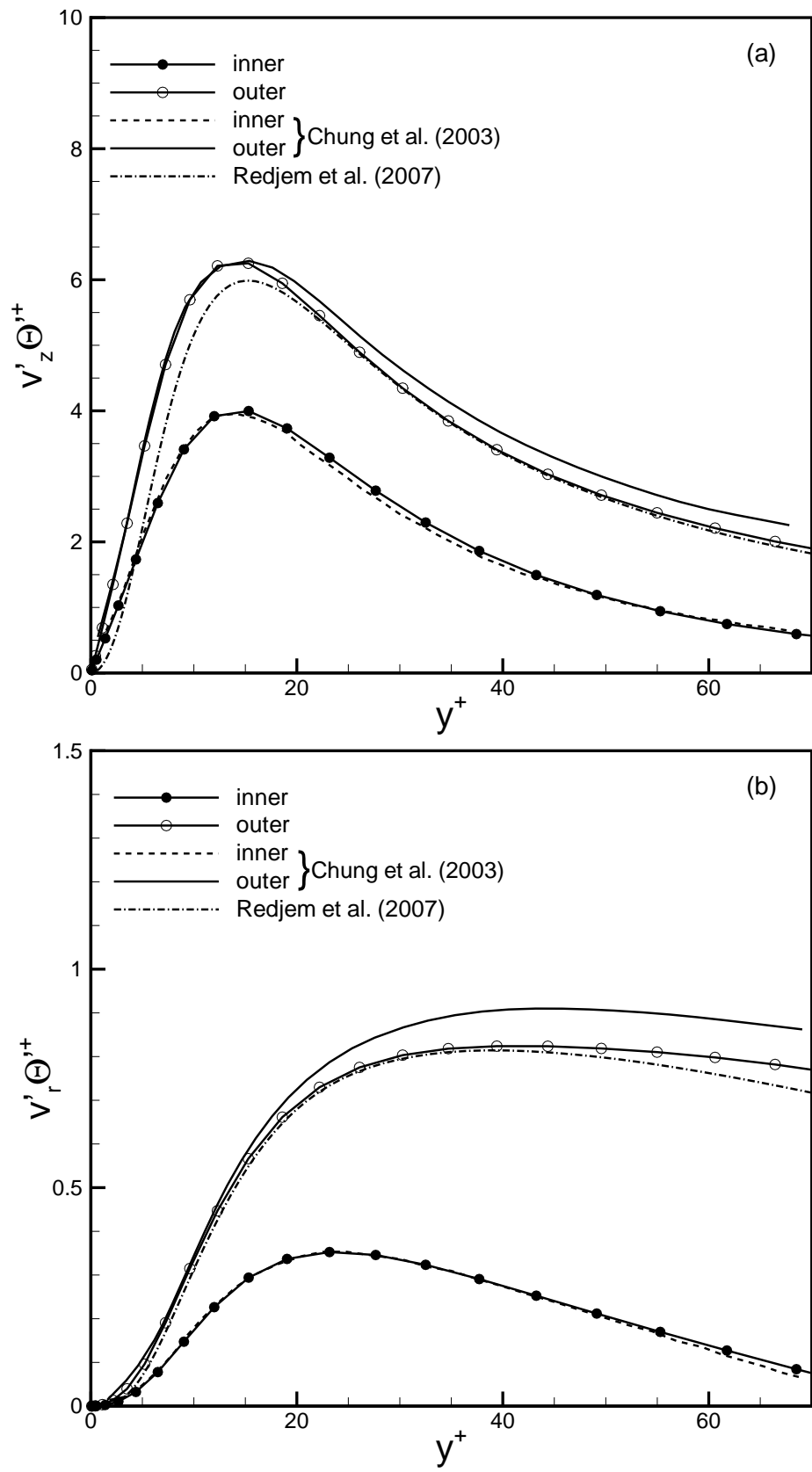


Figure 10: Turbulent heat fluxes for $q^* = 1$. (a) streamwise component, (b) wall-normal component

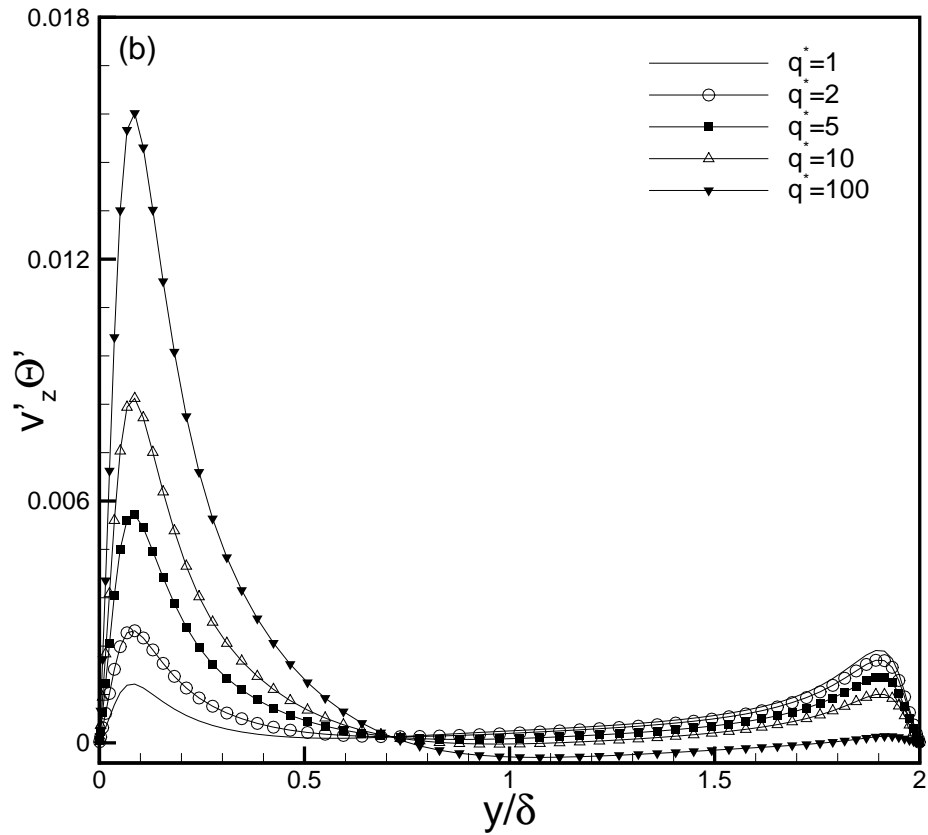
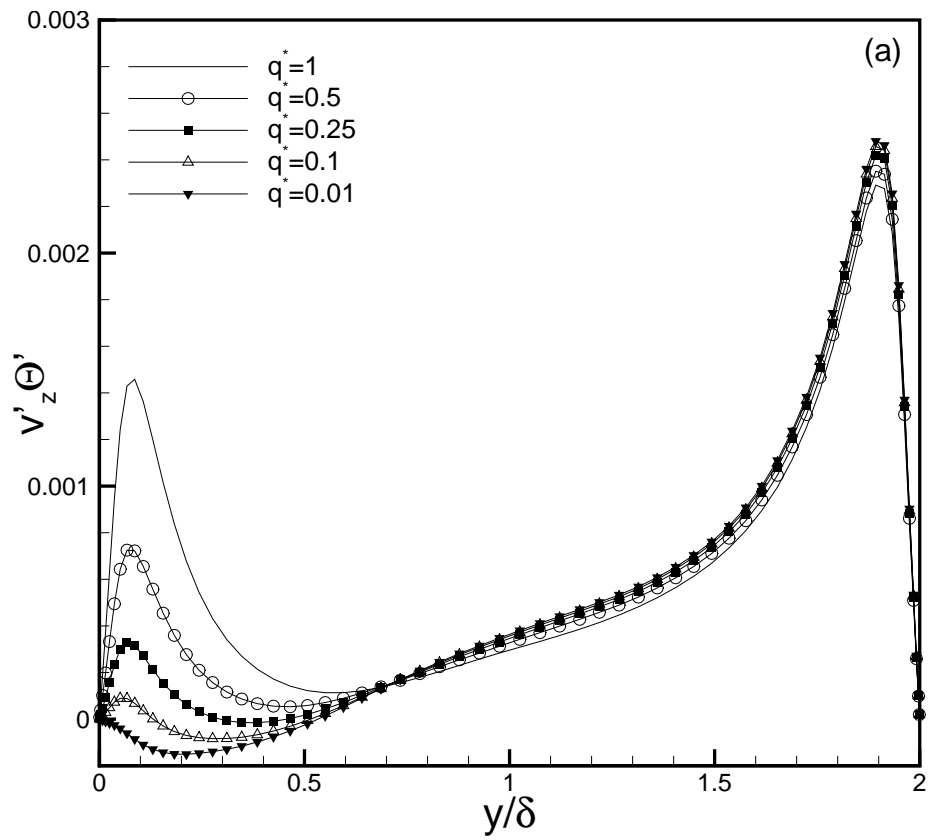


Figure 11: Streamwise turbulent heat flux for various heat flux ratios. (a) $q^* \leq 1$, (b) $q^* \geq 1$

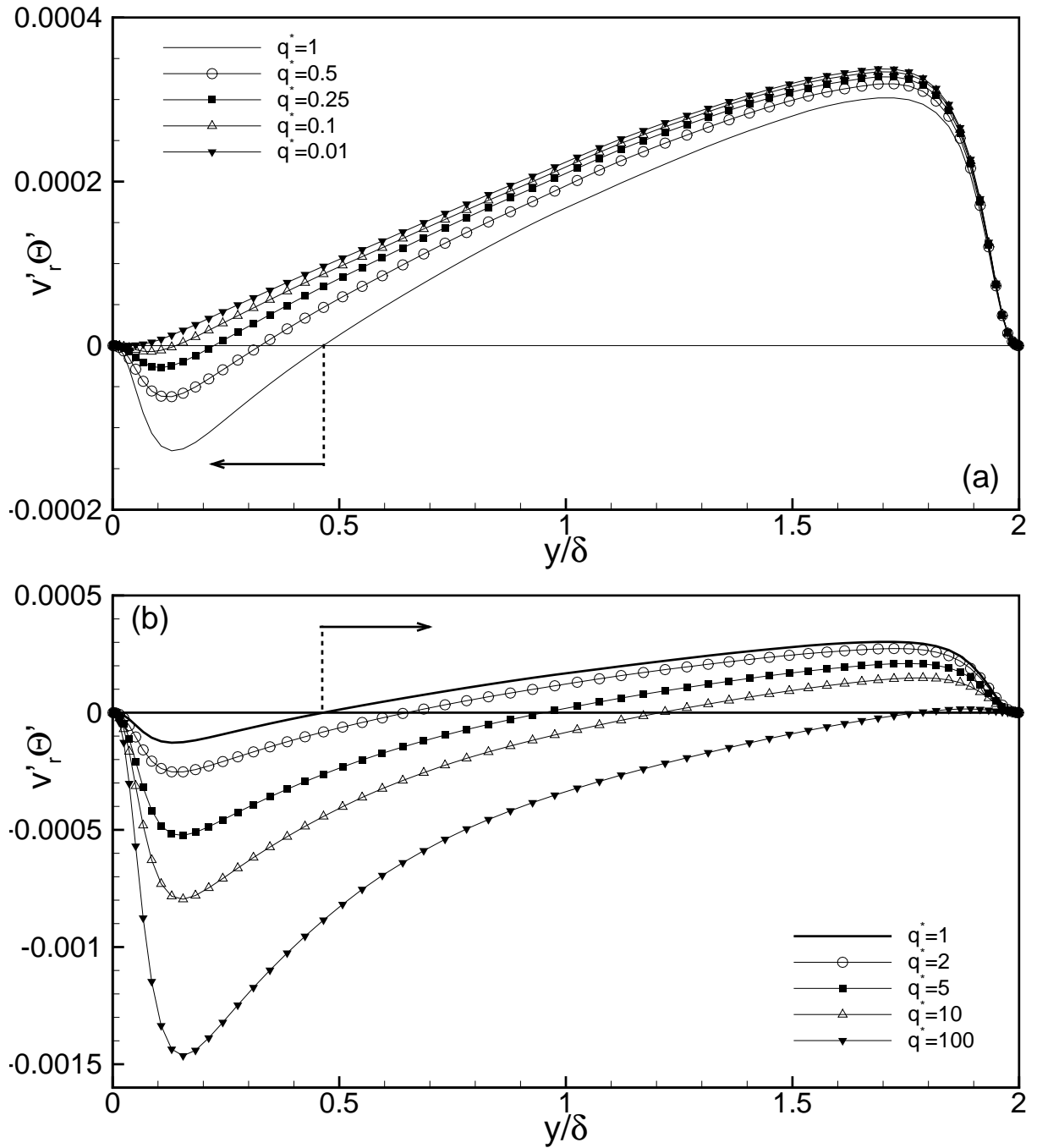


Figure 12: Wall-normal turbulent heat flux for various heat flux ratios. (a) $q^* \leq 1$, (b) $q^* \geq 1$

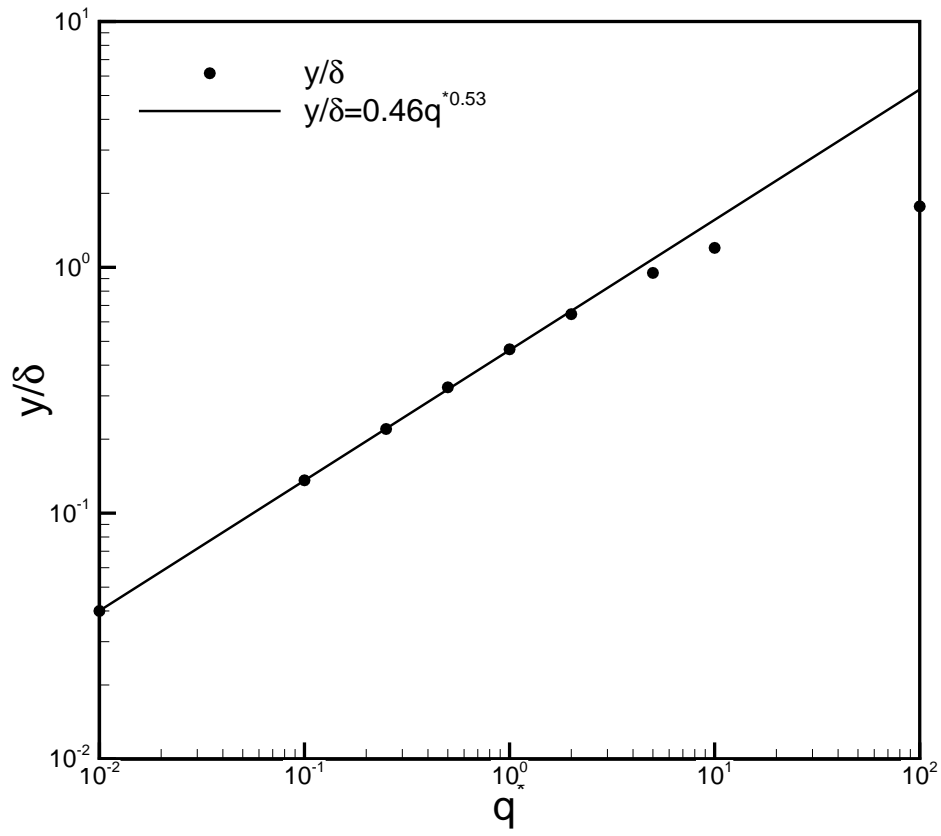


Figure 13: Position of zero wall-normal turbulent heat flux versus heat flux ratio.